*Journal of the European Ceramic Society* **8** (1991) 187–194

# Determination of Preferred Orientation Textures in $Al_2O_3$ Ceramics

A. Böcker, H. G. Brokmeier* & H. J. Bunge

Department of Physical Metallurgy, TU Clausthal,
Grosser Bruch 23, D-3392 Clausthal-Zellerfeld, FRG

(Received 18 January 1991; revised version received 3 April 1991; accepted 12 April 1991)

## Abstract

*Strongly preferred orientation textures are observed in some $Al_2O_3$ ceramics. In these textures the basal plane is parallel to the sheet plane. Textures of this type can be best represented by the basal plane pole figure, i.e. the c-axis distribution. This pole figure is difficult to measure by X-ray diffraction because of a very low structure factor. It can, however, be calculated mathematically from other measured pole figures. The reliability of this procedure was proved with the help of neutron diffraction. In this latter method the structure factor is high enough to measure the basal plane pole figure directly.*

*In einigen $Al_2O_3$-Werkstoffen wird eine ausgeprägte Textur beobachtet. Bei dieser Textur liegt die Basisebene parallel zur Folienebene. Texturen dieses Typs können durch die Polfigur der Basisebene, bzw. der c-Achsenverteilung am besten dargestellt werden. Über die Röntgenbeugung kann diese Polfigur auf Grund des niedrigen Strukturfaktors nur schlecht bestimmt werden. Es ist jedoch möglich, sie aus anderen gemessenen Polfiguren mathematisch abzuleiten. Die Zuverlässigkeit dieses Verfahrens wurde mittels Neutronenbeugung verifiziert. Bei dem letztgenannten Verfahren ist der Strukturfaktor hoch genug, um die Polfigur der Basisebene direkt zu messen.*

*Certaines céramiques $Al_2O_3$ présentent des textures d'orientation préférentielle fortement marquées. Dans ces textures, le plan basal est parallèle au plan de couche. Les textures de ce type peuvent être représentées au mieux par la figure de pôle du plan basal, c'est à dire par la distribution de l'axe c. Cette figure de pôle est difficile à mesurer par diffraction X du fait du très faible facteur de structure. Il peut tout de même être calculé mathématiquement à partir d'autres figures de pôles mesurées. La fiabilité de cette méthode a été vérifiée à l'aide de la diffraction neutronique. Par cette dernière méthode, le facteur de structure est suffisamment élevé pour mesurer directement la figure de pôle du plan basal.*

## 1 Introduction

Preferred orientation of crystallites is the basis for the directional dependence of physical and technological properties of polycrystalline materials. Preferred orientation may originate from all steps of the production process which the material has run through. Directional dependence of macroscopic properties may be advantageous in a material (e.g. high-temperature superconductors) or it may be disadvantageous (e.g. copper-bonded $Al_2O_3$ substrates). In either case it is necessary to measure preferred orientation textures quantitatively and to study the processes of their formation during the production process of the material.

In $Al_2O_3$ sheets preferred orientations of different degrees can be produced, ranging from near to random up to peak densities of 23 × random, as in the present case (and probably even higher). It has also been found that the texture strength strongly influences the properties of these materials, e.g. the thermo-shock behaviour of copper-bonded substrates.[1] Macroscopic anisotropy may generally be observed in all those material properties which are crystallographically anisotropic (e.g. Young's modulus, thermal expansion, fracture toughness and many others). The particular type of texture often found in $Al_2O_3$ sheets is an axially symmetric 'fibre'-texture with the crystallographic *c*-axis perpendicular to the sheet plane. This type of texture

---

* Present address: GKSS Research Establishment, Max-Plank-Strasse, D-2054 Geesthacht, FRG.

*Journal of the European Ceramic Society* 0955-2219/91/$3.50

can be best characterized by the $c$-axis distribution. This latter distribution is, however, difficult to measure by X-ray diffraction because of the low structure factors of all (0001) reflections. The distributions of all other crystal directions, i.e. all other $(hkil)$-pole figures, are rather flat in this case. They reveal the presence of a strong texture only after a quantitative mathematical analysis. Such a texture may be called a 'camouflaged' texture.

There are essentially two ways to determine a camouflaged texture of this type:

(1) To use a quantitative mathematical analysis to calculate the $c$-axis distribution from several other $(hkil)$ distributions.

(2) To measure the $c$-axis distribution directly by neutron diffraction for which the structure factor (0006) is sufficiently high.

It was the purpose of the present study to show that both these methods are equally suitable to determine the 'camouflaged' texture of $Al_2O_3$ sheets.

## 2 Texture Analysis

The texture of a polycrystalline material is defined by the orientation distribution function (ODF) of its crystallites:

$$\frac{\mathrm{d}V/V}{\mathrm{d}g} = f(g) = f(\varphi_1 \Phi \varphi_2)$$
$$\mathrm{d}g = \frac{1}{8\pi^2} \sin\Phi \, \mathrm{d}\varphi_1 \, \mathrm{d}\Phi \, \mathrm{d}\varphi_2 \qquad (1)$$

where $\mathrm{d}V/V$ is the volume fraction of crystallites having the orientation $g$ of their crystal axes (crystal coordinate system $K_B$) with respect to an appropriately chosen sample coordinate system $K_A$, as is shown schematically in Fig. 1,[2] and $\varphi_1$, $\Phi$ and $\varphi_2$ are the orientation angles.

The orientation $g$ of a crystallite may be specified in many different ways, two of which are shown in Fig. 2. The most obvious representation is to specify the crystallographic direction $[hkl]$ parallel to the sample normal direction and the direction $[uvw]$ parallel to a particular direction in the sample surface (Fig. 2(a)). For the purpose of representing continuous orientation distribution functions, however, three independent angular parameters are more appropriate, e.g. the Eulerian angles shown in Fig. 2(b). They are obtained if one starts with the crystal coordinate system $K_B$ parallel to the sample coordinate system $K_A$ and then rotates the crystal successively through $\varphi_1$ about its $z$-axis, through $\Phi$ about its $x$-axis and once more through $\varphi_2$ about its $z$-axis (in its new position). The values of the three Eulerian angles are then plotted as Cartesian coordinates, thus forming the three-dimensional orientation space (i.e. the Euler space) in which the ODF is given by equi-density surfaces or by equi-density lines in two-dimensional sections of this space (see e.g. Fig. 9). The orientation density values are normalized in multiples of the random orientation density.

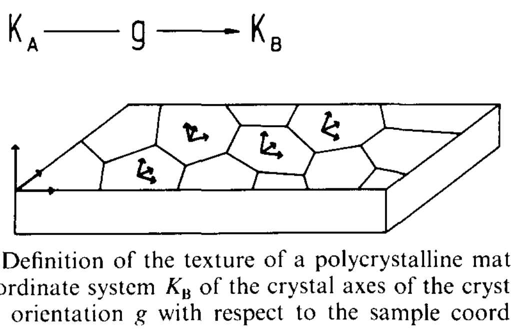

**Fig. 1.** Definition of the texture of a polycrystalline material. The coordinate system $K_B$ of the crystal axes of the crystallite has the orientation $g$ with respect to the sample coordinate system $K_A$.

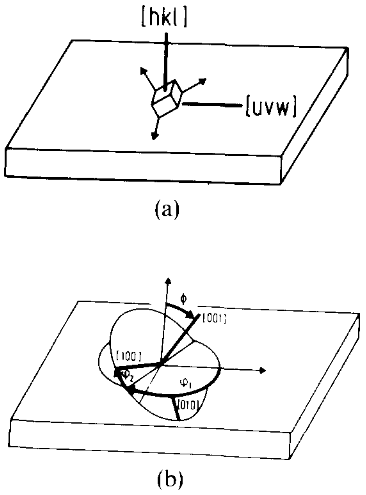

**Fig. 2.** Two specifications of crystal orientation $g$: (a) Miller indices $[hkl][uvw]$ and (b) Euclerian angles $\{\varphi_1, \Phi, \varphi_2\}$.

The orientation distribution function eqn (1) can—in principle—be determined by measuring the orientation angles $\varphi_1$, $\Phi$ and $\varphi_2$ of each crystallite separately (e.g. by electron diffraction). This is, however, difficult and time consuming. The most common way to determine the ODF is to measure the angular distribution of particular crystal directions, i.e. the normal directions to reflecting lattice planes $(hkl)$ (Fig. 3), by X-ray or neutron diffraction.[3]

$$\frac{\mathrm{d}V/V}{\mathrm{d}\Omega} = P_{(hkl)}(\alpha\beta)$$
$$\mathrm{d}\Omega = \sin\alpha \, \mathrm{d}\alpha \, \mathrm{d}\beta \qquad (2)$$

where $\mathrm{d}V/V$ is the volume fraction of crystallites of which the normal direction to the lattice plane $(hkl)$

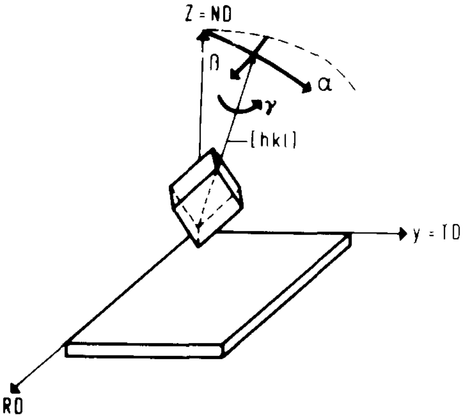

**Fig. 3.** Angular coordinates $\{\alpha,\beta\}$ of a particular crystal direction (normal to the lattice plane $(hkl)$) with respect to the sample coordinate system.

is parallel to the sample direction with the polar coordinates $\{\alpha,\beta\}$ within a solid angular element, $d\Omega$ (Fig. 4). This pole density distribution function or pole 'figure' can easily be measured in the back-reflection range (Fig. 5) using a texture goniometer.

The pole figure is an integral (two-dimensional projection) over the orientation distribution function

$$P_{(hkl)}(\alpha\beta)=\frac{1}{2\pi}\int_{(hkl)\perp(\alpha\beta)} f(\varphi_1\Phi\varphi_2)\,d\gamma \qquad (3)$$

The diffraction process does not 'see' a rotation $\gamma$ of any crystallite about the normal direction to the reflecting lattice plane (see Fig. 3). If several pole figures $P_{(hkl)}(\alpha\beta)$ from different lattice planes $(hkl)$ are available, then the three-dimensional distribution function $f(\varphi_1,\Phi,\varphi_2)$ can be calculated by solving eqn (3).[2] This procedure is called 'pole figure inversion' and is comparable to computer tomography (only it is applied to the orientation space rather than to the real space).

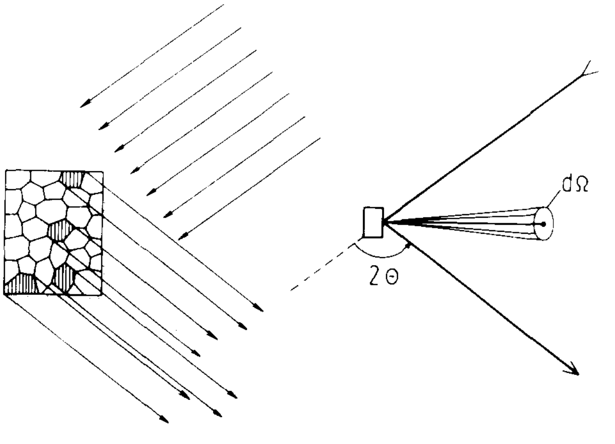

**Fig. 4.** The reflected intensity is proportional to the volume fraction of crystallites in reflection position.

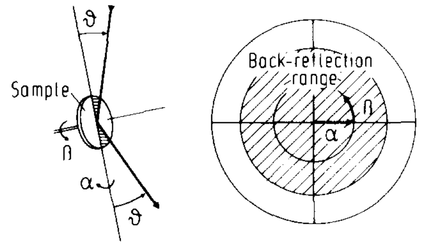

**Fig. 5.** Pole figure measurement by scanning the sample through the angles $\{\alpha,\beta\}$.

Several mathematical algorithms for pole figure inversion have been published.[3] The most frequently used one is that by series expansion of both functions, i.e. the ODF $f(g)$ and the pole figures $P_{(hkl)}(\alpha,\beta)$, in the form

$$f(\varphi_1\Phi\varphi_2)=\sum_{\lambda=0}^{L}\sum_{\mu=1}^{M(\lambda)}\sum_{\nu=1}^{N(\lambda)} C_\lambda^{\mu\nu}\overset{:\cdot}{T}{}_\lambda^{\mu\nu}(\varphi_1\Phi\varphi_2) \qquad (4)$$

$$P_{(hkl)}(\alpha\beta)=\sum_{\lambda=0}^{L}\sum_{\mu=1}^{M(\lambda)}\sum_{\nu=1}^{N(\lambda)} C_\lambda^{\mu\nu}\frac{4\pi}{2\lambda+1}\overset{:}{K}{}_\lambda^{\mu}(hkl)\dot{K}_\lambda^{\nu}(\alpha\beta) \qquad (5)$$

where $\overset{:}{K}{}_\lambda^{\mu}(hkl)$ and $\dot{K}_\lambda^{\nu}(\alpha\beta)$ are symmetrized spherical harmonic functions depending on the crystal direction perpendicular to the lattice plane $(hkl)$ and sample direction $\{\alpha,\beta\}$ respectively. They are invariant with respect to crystal symmetry, symbolized by : above the functional symbol $K$, or to sample symmetry, symbolized by ·, respectively. The functions $\overset{:\cdot}{T}$ are generalized harmonic functions which are invariant to both these symmetries.[2] The maximum series expansion degree $L$ must be appropriately chosen. It must be higher the 'stronger' the texture. The texture is then completely characterized by the set of coefficients $C_\lambda^{\mu\nu}$.

The pole density distribution functions in eqn (2) can be measured by X-ray or neutron diffraction using a texture goniometer which allows the placing of a detector at the diffraction angle $\Theta$, Fig. 4, and the rotation of the sample through the angles $\{\alpha,\beta\}$, Fig. 5. Then the measured intensity is given by

$$I_{\Theta_{(hkl)}}(\alpha\beta)=I_0\,.\,A\,.\,R_{(hkl)}\cdot P_{(hkl)}(\alpha\beta) \qquad (6)$$

where $I_0$ is the intensity of the incident beam, $A$ is some factor depending on the experimental conditions (including sample size) and $R_{(hkl)}$ is the reflectivity of the lattice plane $(hkl)$. Generally the reflectivity is different for X-ray and neutron diffraction.[4]

For the sake of a convenient measurement lattice planes with the strongest $R$-values are mostly chosen. In some cases (as in the one discussed in this paper) the strongest reflections $(hkl)$ are not the most informative ones from the viewpoint of pole density distribution $P_{(hkl)}(\alpha, \beta)$.[1] It is then possible to use the strongest reflections to solve eqn (3) and thus to obtain the coefficients $C_\lambda^{\mu\nu}$. From these coefficients any other pole density function can be calculated using eqn (5). In the present paper this procedure is used to calculate the pole density distribution of the *c*-axis normal to the basal plane (0001) which has very weak *R*-values in the case of X-ray diffraction (not, however, for neutron diffraction).

It is not always necessary to calculate the complete orientation distribution function in order to estimate the texture of a sample. Texture analysis can thus be done in three 'levels' of increasing accuracy:

(1) For a rough inspection of the texture it is sufficient to measure a diffraction spectrum $I(\theta)$ for *one* sample direction $\{\alpha, \beta\}$, e.g. the sample normal direction $\alpha = 0$ and to consider the deviation of the measured intensity from the corresponding one of a random sample $I^{\mathrm{rand}}(\theta)$ which is contained in the values $R_{(hkl)}$. This can be done with a standard powder diffractometer.

(2) A more quantitative result can be obtained by measuring one or more pole 'figures' $P_{(hkl)}(\alpha, \beta)$ as a function of the sample angles $\{\alpha, \beta\}$. This requires a texture goniometer on which the sample can be tilted and rotated through the angles $\{\alpha, \beta\}$.

(3) The most comprehensive method, however, is to calculate the ODF $f(\varphi_1, \Phi, \varphi_2)$ from several pole figures by solving eqn (3).

## 3 Experimental Procedure

The material used was $Al_2O_3$ in sheets of 0·6 mm thickness obtained after a particular green-forming and firing process.

X-ray texture measurements were carried out by a back-reflection technique using the automatic texture goniometer ATEMA-C and $\mathrm{Co}K_{\bar{\alpha}}$ radiation. Pole figures were measured in steps of $\Delta\alpha = 5°$ and $\Delta\beta = 3{\cdot}6°$ in the back-reflection ranges $0° \leq \alpha \leq 70°$ and $0° \leq \beta \leq 360°$. Four pole figures were measured, i.e. $(10\bar{1}4)$, $(02\bar{2}4)$, $(11\bar{2}6)$, $(11\bar{2}3)$. The measuring time per pole figure point was $\simeq 3{\cdot}6$ s.

From these pole figures the texture coefficients $C_\lambda^{\mu\nu}$ were calculated by solving eqn (3) using a computer program for incomplete pole figures. In this method, the coefficients for odd values of $\lambda$ are obtained with the positivity method.[5] From the coefficients $C_\lambda^{\mu\nu}$ the texture function $f(\varphi_1, \Phi, \varphi_2)$ was calculated in steps of $\Delta\varphi_1 = \Delta\Phi = \Delta\varphi_2 = 5°$ in the assymmetric range $0° \leq \varphi_1 \leq 90°$, $0° \leq \Phi \leq 90°$ and $0° \leq \Phi_2 \leq 60°$. The

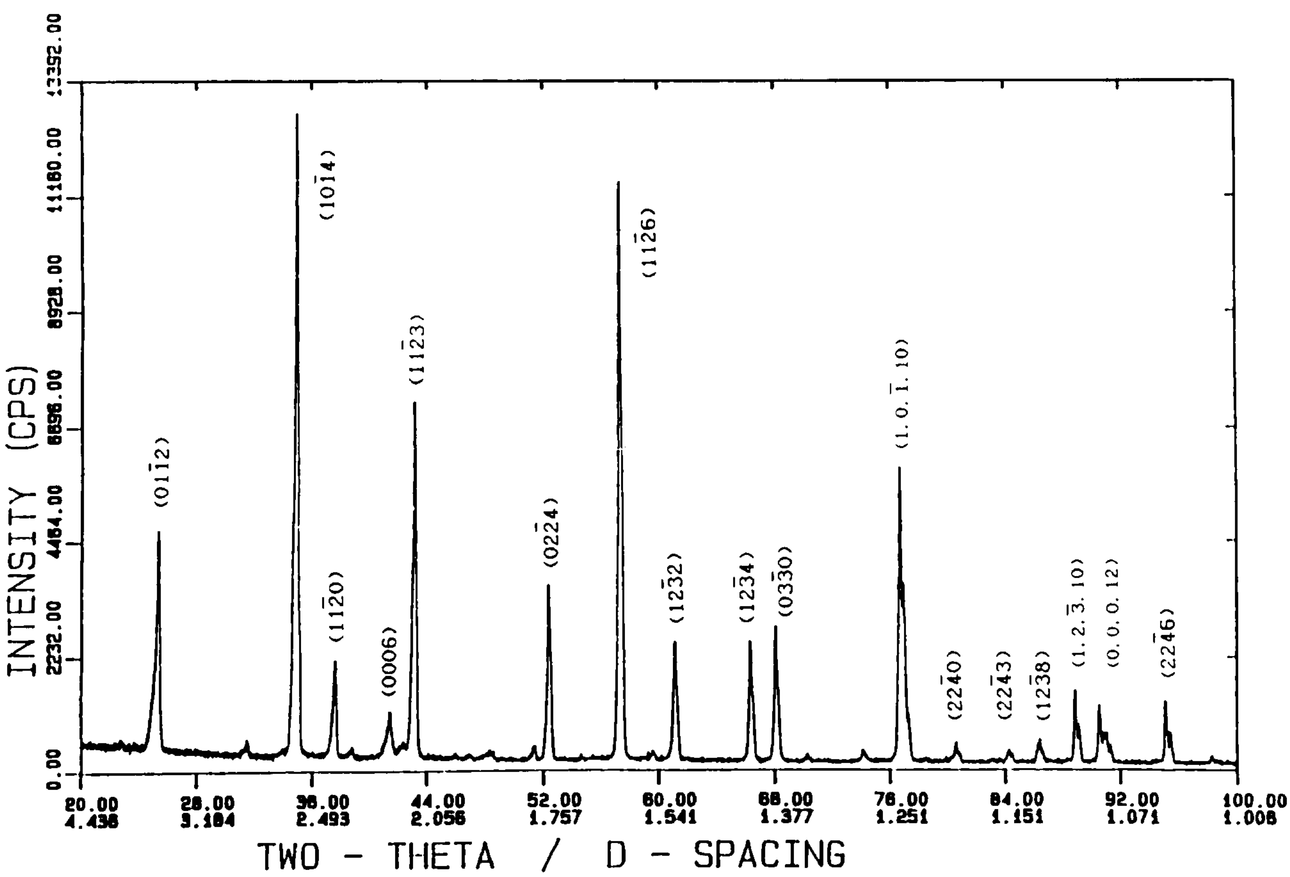

**Fig. 6.** The X-ray diffraction spectrum of $Al_2O_3$ for $\mathrm{Cu}K_{\bar{\alpha}}$ radiation.

calculated $f$-values are interpolated by equi-level lines expressed in multiples of the random orientation density. Additionally, the $c$-axis pole figure (0001) was also calculated from the coefficients $C_\lambda^{\mu\nu}$.

Neutron diffraction texture measurements were carried out with the texture goniometer TEX-2 installed at the research reactor FRG-1 at Geesthacht. Measurements were done with the wavelength $\lambda = 1{\cdot}168$ in steps of $\Delta\alpha = 5°$ in the range $0° \leq \alpha \leq 90°$; axial symmetry known from X-ray diffraction was presumed, but also tested by measuring the complete (10$\bar{1}$4) pole figure in steps of $\Delta\alpha = 5°$ and $\Delta\beta = 3{\cdot}6°$. In this case the following pole figures were measured: (10$\bar{1}$4), (02$\bar{2}$4), (11$\bar{2}$6), (11$\bar{2}$3), (01$\bar{1}$2), (11$\bar{2}$0), (0006). Measuring time per pole figure point was 360 s. Also in this case, the ODF $f(g)$ was calculated using the same series expansion method.

## 4 Results

### 4.1 X-Ray diffraction

The $2\theta$ diffraction spectrum taken perpendicular to the sample plane is shown in Fig. 6 for $CuK_\alpha$ radiation. In this sample orientation the (0006) reflection takes on its maximum intensity. Hence, it is visible in the spectrum, but its intensity is not sufficient for measurement of a pole figure with the required accuracy in due time.

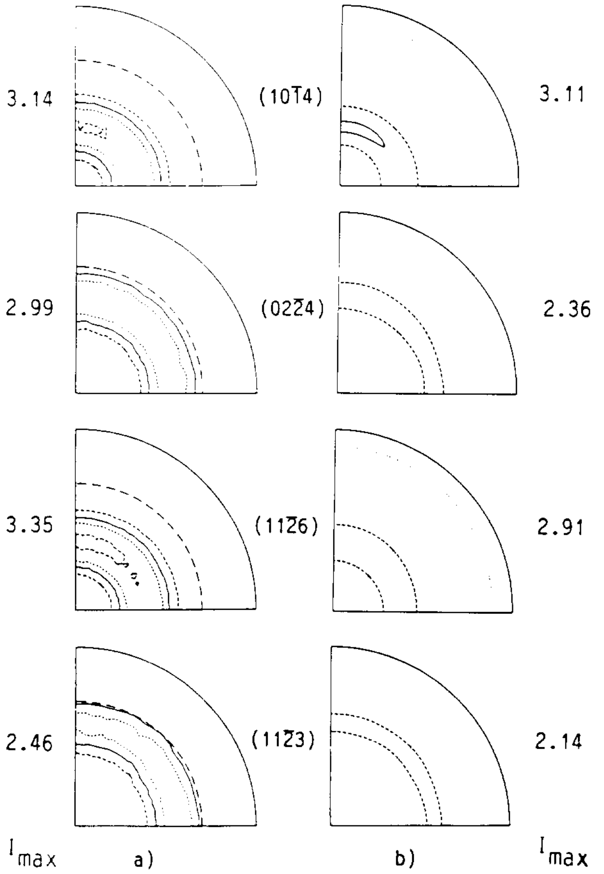

**Fig. 7.** Pole figures of an $Al_2O_3$ sheet: (a) measured incomplete pole figures and (b) recalculated complete pole figures.

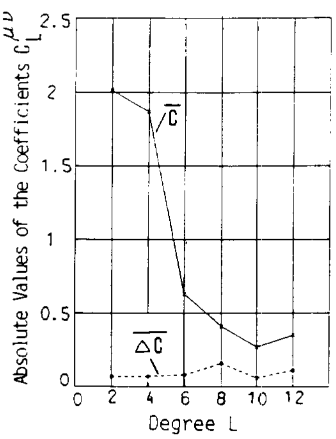

**Fig. 8.** Mean absolute values of the coefficients $C_\lambda^{\mu\nu}$ (averaged over $\mu$ and $\nu$) and the respective error quantities.

The measured pole figures are shown in Fig. 7(a). They are pseudo-normalized in multiples of the random orientation density, i.e. normalized only on the basis of the measured range $\alpha \leq 70°$. It is seen that the maximum pole densities are less than 3·35 × random. From these pole figures the coefficients $C_\lambda^{\mu\nu}$ were calculated. The mean absolute values, $\bar{c}$, of these coefficients, averaged over $\mu$ and $\nu$, are shown in Fig. 8 together with their respective error values $\Delta\bar{c}$. This curve is used to estimate the convergence of the series expansion. The orientation distribution function was then calculated with $\lambda_{max} = 12$. It is

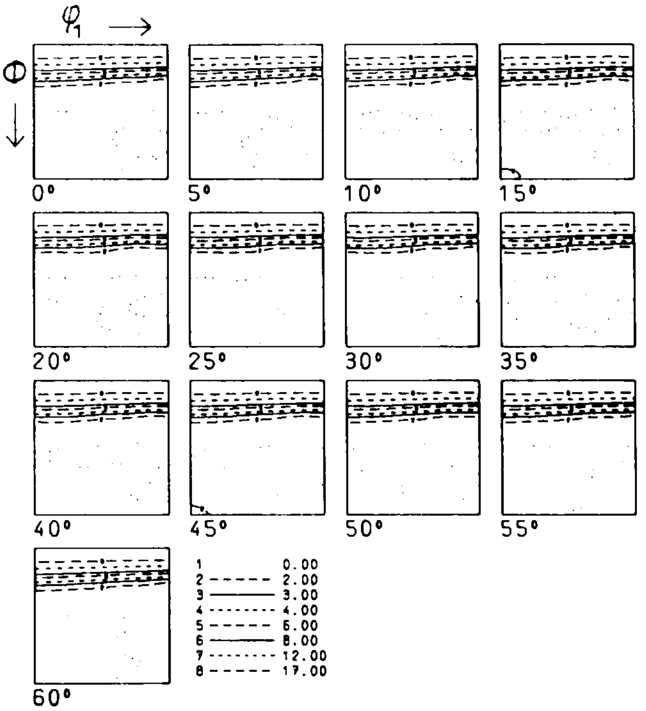

**Fig. 9.** The orientation distribution function ODF calculated from the pole figures of Fig. 7. The function is expressed by equi-level lines in multiples of the random density. The individual sections correspond to constant values of the angle $\varphi_2 = 0$ (5°) 60%.

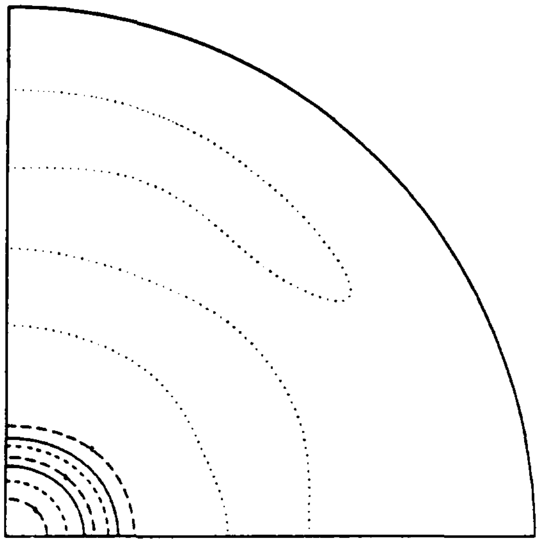

**Fig. 10.** The basal (0006) plane pole figure calculated from the coefficients $C_\lambda^{\mu\nu}$.

shown in Fig. 9 in sections $\varphi_2 = \text{const.}$ It can be seen that in this function the maximum orientation density rises to $\simeq 23\times$ random.

The basal plane pole figure calculated from $C_\lambda^{\mu\nu}$ with $\lambda_{\max} = 12$ is shown in Fig. 10. This function also rises to $\simeq 23\times$ random (see Table 1). In order to estimate the reliability of the calculated coefficients $C_\lambda^{\mu\nu}$ the measured pole figures were also recalculated from the texture coefficients. They can be compared directly with the measured values, as is shown in Fig. 7(b).

## 4.2 Neutron diffraction

Neutron diffraction was mainly used to check the X-ray results. Table 1 gives the maximum pole densities measured in the different pole figures using X-rays and neutrons, respectively. The agreement between both methods is quite satisfactory. In contrast to using X-ray diffraction, it is possible, using neutron diffraction, to measure the basal plane pole figure (0006). The result is shown in Fig. 11. This figure also contains the corresponding recalculated curve which was obtained with the maximum expansion degree $\lambda_{\max} = 22$. Furthermore, the two curves are compared with the corresponding one obtained by X-ray diffraction. From texture coefficients $C_\lambda^{\mu\nu}$ the so-called inverse pole figures can also be calculated.[2,3] They are obtained by eqn (5) if the sample direction $\{\alpha, \beta\}$ is kept constant and the crystal direction

**Table 1.** Maximum pole densities of various lattice planes measured by X-ray and neutron diffraction

| *Lattice plane* | *Maximum pole density* | |
|---|---|---|
| | *X-Rays* | *Neutrons* |
| (1014) | 3·14 | 3·50 |
| (0224) | 2·99 | 2·30 |
| (1126) | 3·35 | 2·90 |
| (1123) | 2·46 | 2·20 |
| (0112) | — | 2·00 |
| (1120) | — | 1·80 |
| (0006) | (22·86) (calc.) | 24·80 |

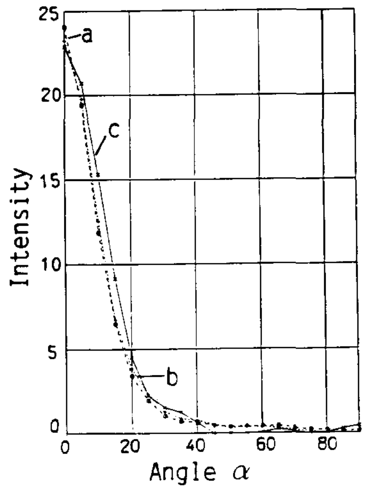

**Fig. 11.** One-dimensional section through the basal plane pole figure: a, measured by neutron diffraction; b, calculated from neutron diffraction; c, calculated from X-ray diffraction. Values in multiples of the random density.

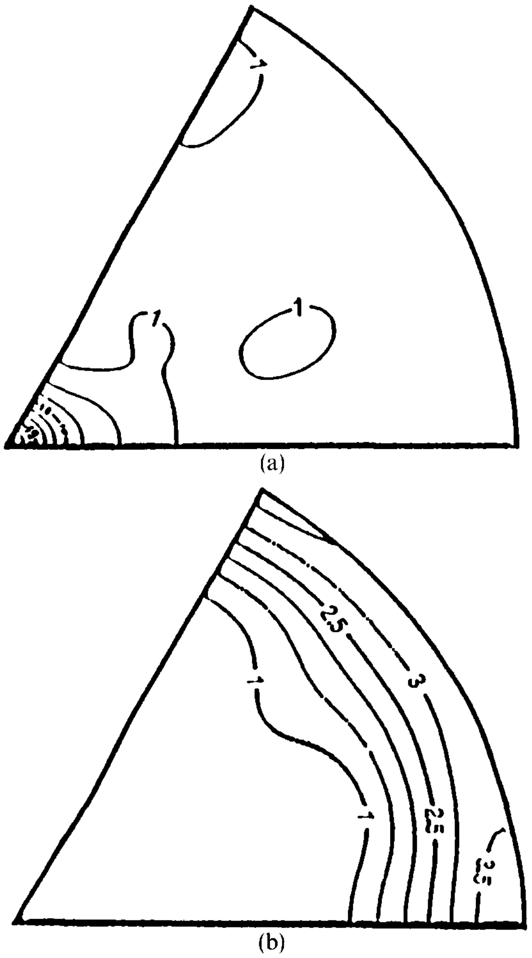

(a)

(b)

**Fig. 12.** Inverse pole figures calculated from texture coefficients $C_\lambda^{\mu\nu}$ on the basis of neutron diffraction. (a) Sheet normal direction; (b) sheet plane direction.

perpendicular to (*hkl*) is taken as a variable. The inverse pole figure thus gives the distribution of crystal directions in a particular sample direction. Inverse pole figures were calculated for the two main sample directions, i.e. the sheet normal direction and a direction in the sheet plane (all directions in this plane are equivalent because of the observed axial symmetry). The two inverse pole figures are given in Fig. 12. The inverse pole figure of normal direction rises up to 23·48 × random, the same value as that of the (0006) pole figure and the ODF, whereas the sheet plane inverse pole figure rises only to a maximum value of 3·74.

## 5 Discussion

The $Al_2O_3$ ceramic studied here exhibits a rather strongly preferred orientation with the crystallographic *c*-axis perpendicular to the sheet plane. The texture is nearly axially symmetric with respect to the sheet normal direction (this has been called a 'fibre' texture). It is also nearly axially symmetric about the crystallographic *c*-axis. In general these two symmetries are independent of each other. With the *c*-axis parallel to the normal direction, however, they are virtually indistinguishable. A texture of this type can be characterized by the *c*-axis pole figure, i.e. the distribution of *c*-axes with respect to the sample coordinate system. Furthermore, with the axial symmetry about this direction a one-dimensional section through this pole figure in the $\alpha$-direction is sufficient to represent this texture. Unfortunately, the *c*-axis distribution cannot be measured by X-ray diffraction because of the low value of the (0001) structure factors. This was called a 'camouflaged' texture.

It is, however, possible to calculate the *c*-axis distribution starting from pole density values of several other reflections (*hkil*). Hence, the relevant information about the texture is implicitly contained in the intensity distributions of these other reflections from which it can be extracted mathematically. This procedure is thus based on small differences of intensity values in these pole figures. The relative accuracy of such difference values is lower than that of the individual pole density values. Hence, the 'extrapolated' (0006) pole figure must have a lower accuracy than a directly measured one. This is especially true when the calculated pole figure has so much higher values than the measured pole figures. It was found that the reliability of the mathematical procedure depends on the appropriate choice of the degree of series expansion $\lambda_{max}$. If $\lambda_{max}$ is chosen too low then essential features of the texture are 'blurred out' by the series truncation effect, i.e. the (0006) pole figure is flattened out and does not reach the correct maximum density values. If, on the other hand, $\lambda_{max}$ is chosen too high then the mathematical procedure becomes instable and produces 'artefacts' in the calculated distribution function. By several tests it was thus found that the value $\lambda_{max} = 12$, used in the calculation based on X-ray diffraction, was the optimum compromise. In the case of neutron diffraction the situation is different. In this case the number of pole figures was 7 and, what is even more important, the critical (0006) pole figure was included in the starting data. Hence, in this case, $\lambda_{max} = 22$ could be used without producing 'oscillations' in the calculated ODF. The measured and calculated (0006) pole figures in Fig. 11 are thus in quite good agreement. Neutron diffraction is, however, much more expansive than X-ray diffraction and also the access to neutron 'beam time' is limited. Hence, routine measurements of textures in materials research programs must be done with X-ray diffraction. It was thus the purpose of the present investigation to prove the accuracy of the (0006) pole figure 'extrapolated' from other X-ray pole figures with direct measurements of this pole figure on the basis of neutron diffraction. This is best seen in the one-dimensional section through the (0006) pole figure shown in Fig. 11. In this figure the curve calculated from X-ray data is compared with the one measured by neutron diffraction as well as with the one calculated from neutron diffraction. It is seen that the X-ray curve corresponds quite well with the directly measured neutron curve. It can thus be concluded that the mathematical procedure based on X-ray pole figures gives reliable results.

## 6 Conclusions

$Al_2O_3$ ceramic sheets can develop strongly preferred orientation textures depending on details of the production process.

A basal plane texture of 23 × random has been observed in the present case. Textures of this type are best represented in the basal plane pole figure which is, however, difficult to measure by X-ray diffraction because of a very low structure factor ('camouflaged' texture).

The basal plane pole figure can be calculated along with the complete orientation distribution function when several other pole figures have been measured. This procedure leads to quite satisfactory and reliable results as was proved with neutron diffraction. Using neutron diffraction, the basal plane pole figure can be measured directly, since the neutron structure factor (0006) is much higher than the corresponding X-ray structure factor.

## Acknowledgement

The neutron diffraction part of this work was funded by the German Federal Ministry Research and Technology (BMFT) under the contract number 03 Bu 2 CLA. The authors further acknowledge valuable cooperation with the companies DODUCO and Hoechst CeramTec.

## References

1. Klein, H., Waibel, B., Martin, M. & Bunge, H. J., Reliability of copper metallized $Al_2O_3$ substrates during thermal cycling as a consequence of preferred orientation (texture). In *Joining Ceramics, Glass and Metal*, ed. W. Kraft. DGM Informationsgesellschaft Oberursel, 1989, pp. 285–90.
2. Bunge, H. J., *Texture Analysis in Materials Science*. Butterworths, London, 1982.
3. Bunge, H. J., Three-dimensional texture analysis. *Intern. Materials Rev.*, **32** (1987) 265–91.
4. Bunge, H. J., Advantages of neutron diffraction texture analysis. *Textures and Microstructures*, **10** (1989) 265–308.
5. Dahms, M. & Bunge, H. J., The iterative series expansion method for quantitative texture analysis. *J. Appl. Cryst.*, **22** (1989) 439–47.